Rapid Communications

Role of cluster structure in the breakup of ^{7}Li

D. Chattopadhyay,[1,2,*] S. Santra,[1,2] A. Pal,[1,2] A. Kundu,[1,2] K. Ramachandran,[1] R. Tripathi,[2,3] B. J. Roy,[1,2] T. N. Nag,[2,3] Y. Sawant,[1] B. K. Nayak,[1,2] A. Saxena,[1,2] and S. Kailas[1,2]

[1]*Nuclear Physics Division, Bhabha Atomic Research Centre, Mumbai 400085, India*

[2]*Homi Bhabha National Institute, Anushakti Nagar, Mumbai 400094, India*

[3]*RadioChemistry Division, Bhabha Atomic Research Centre, Mumbai 400085, India*

(Received 12 April 2018; published 31 May 2018)

Direct and sequential breakups of the projectile in the ^{7}Li + ^{112}Sn reaction have been measured at a beam energy of 30 MeV. Cross sections for sequential breakup of ^{7}Li into α and t cluster fragments via its second resonant state of $5/2^{-}$ (6.68 MeV) in the continuum have been measured for the first time along with the first resonant state ($7/2^{-}$, 4.63 MeV). Probabilities of sequential breakup proceeding through $-1n$ and $-2n$ transfer channels, i.e., (^{7}Li,^{6}Li) and (^{7}Li,^{5}Li) reactions followed by breakup, into $\alpha + d$ and $\alpha + p$, respectively, were found to dominate over $\alpha + t$ breakup. Measured cross sections for the above breakup channels and elastic scattering have been compared with coupled-channel calculations to understand the reaction mechanism involving the weakly bound projectile ^{7}Li. Significant cross section for direct breakup of $^{7}\mathrm{Li} \rightarrow {}^{6}\mathrm{He} + p$ has also been measured for the first time, indicating the importance of the new (^{6}He + p) cluster configuration that may be necessary to understand the complete structure of ^{7}Li and its energy levels.

DOI: 10.1103/PhysRevC.97.051601

Study of projectile breakup in the field of a target nucleus is a topic of increasing interest [1–4], particularly due to recent advent of the availability of weakly bound exotic beams. Measurements for direct and sequential breakup cross sections in reactions involving weakly bound stable projectiles having $\alpha + x$ cluster structures like ^{6,7}Li and ^{9}Be are available in the literature [5–17] but on very few heavy and light targets. Investigation of sequential breakup in the above reactions through new resonance states and/or transfer channels is a matter of great interest for detailed understanding of the breakup reaction mechanism. In our recent work [5], systematic measurement of direct as well as sequential breakup cross sections for different outgoing channels in a reaction involving ^{6}Li with a medium mass target ^{112}Sn has been reported. In addition to several well-known breakup channels, a new breakup channel for ^{6}Li breaking into α and d via its third resonance state (1^{+}, 5.65 MeV) was observed. The use of large detector array with wide angular coverage has made it possible to measure the higher resonance states. With similar motivations and using even a bigger detector array, a reaction involving the same ^{112}Sn target but with a different weakly bound projectile, i.e., ^{7}Li was chosen for the present work.

The cluster structure of a light nucleus plays an important role in predicting possible breakup channels. The ^{7}Li as a cluster of α and t with a binding energy of only 2.47 MeV is very well known. Direct breakup of ^{7}Li into $\alpha + t$ and sequential breakup via the first resonance state ($7/2^{-}$, 4.63 MeV) of the cluster have been measured for several systems. But there is no measurement available on the sequential breakup corresponding to the second resonance state ($5/2^{-}$, 6.68 MeV). The study of this state is, however, very important because various studies on elastic scattering show a significant effect of coupling of the $5/2^{-}$ state of ^{7}Li [18,19]. So, it would be interesting to measure this new channel to better understand the mechanism of $\alpha + t$ resonance breakup.

Cluster models of the structure of light nuclei frequently provide a rather simple description of some of the energy levels which are difficult to access in the usual shell-model framework. The model described in Ref. [20] is used to study the low-lying energy levels of ^{7}Li, whose structure is treated as a superposition of the clusters $\alpha + t$ and $^{6}\mathrm{Li} + n$ with binding energies of 2.47 and 7.25 MeV, respectively. Other possible cluster structures like $^{6}\mathrm{He} + p$ were not considered because of its high binding energy (∼9.96 MeV). Investigation of the breakup channel $^{7}\mathrm{Li} \rightarrow {}^{6}\mathrm{He} + p$ will shed light on the possibility of the third cluster structure of ^{7}Li.

In addition, the transfer breakup channels are known [21] to play a very important role in understanding the large cross sections for inclusive α particles. Apart from $\alpha + t$ breakup, the α particles can be produced by transfer triggered breakup. For example, the transfer reactions of (^{7}Li,^{6}Li), (^{7}Li,^{5}Li), (^{7}Li,^{8}Be), (^{7}Li,^{6}He), and (^{7}Li,^{5}He) followed by breakup into $\alpha + d$, $\alpha + p$, $\alpha + \alpha$, $\alpha + 2n$, and $\alpha + n$, respectively, can contribute individually to the inclusive α production.

In this Rapid Communication, we report the results of experimental investigation of the existence of (i) ^{7}Li breakup into $\alpha + t$ via its second as well as first resonance state and (ii) direct breakup of ^{7}Li into $^{6}\mathrm{He} + p$. In addition, the breakup induced by $-1n$ transfer and $-2n$ transfer has also been investigated. Experimental cross sections have been compared with the results of coupled-channel calculations.

Coincidence measurements have been carried out for the $^{7}\mathrm{Li} + {}^{112}\mathrm{Sn}$ system at a beam energy $E_{\mathrm{beam}} = 30$ MeV,

*dipayanchattopadhyay90@gmail.com

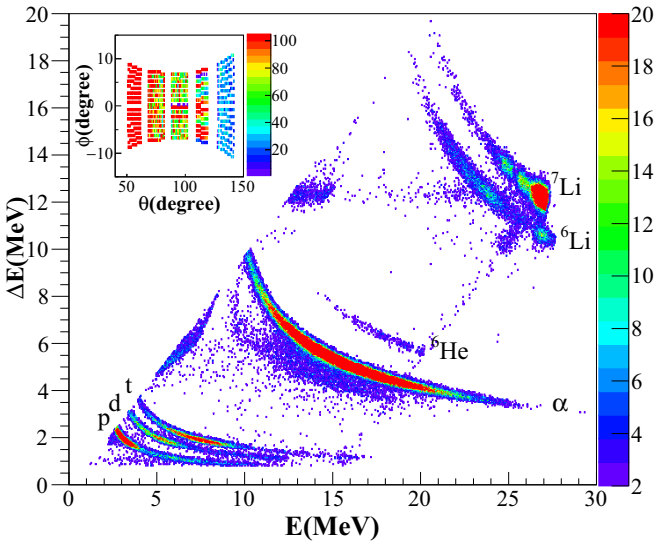

FIG. 1. Typical two-dimensional (ΔE vs $E_{\rm total}$) energy-calibrated spectrum acquired in one of the vertical strips at $\theta = 70^\circ$ for a beam energy of 30 MeV. The inset shows the total coverage in θ and ϕ by the strip detector array, and the intensity represents the number of α particles detected in coincidence with t, d, or p in any two vertical strips.

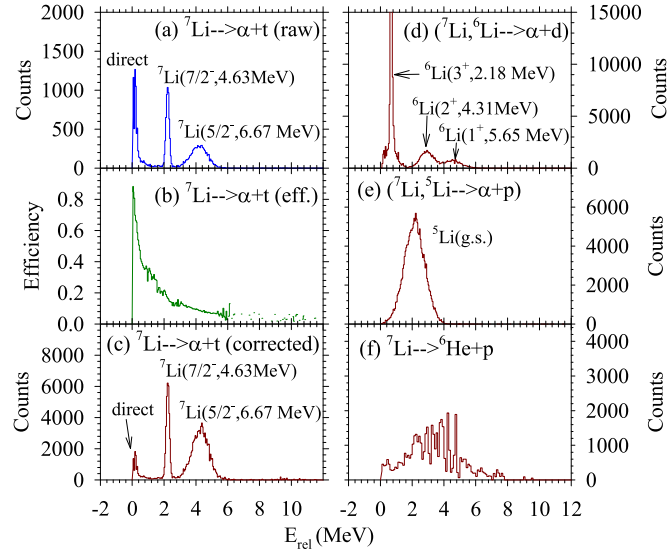

FIG. 2. [Left panel] For $\alpha + t$ breakup: (a) $E_{\rm rel}$ distribution without efficiency correction, (b) efficiency of the detector array, and (c) efficiency-corrected $E_{\rm rel}$ distribution. [Right panel] The efficiency-corrected $E_{\rm rel}$ distributions corresponding to (d) $\alpha + d$ breakup, (e) $\alpha + p$ breakup, and (f) ^{6}He + p breakup. The $E_{\rm rel}$ bin size in the histogram (f) is 0.1 MeV which is double of that in (d) and (e).

using the 14-UD Pelletron-Linac facility in Mumbai. A self-supporting enriched (>99%) ^{112}Sn foil of thickness $\sim$540 μg/cm^2 was used as a target. The corrected beam energy with the loss in half target thickness is $\approx$29.8 MeV ($E_{\rm c.m.}/V_b \sim 1.37$). An array of five strip telescopes (S_1–S_5) with large angular coverage, $\sim$93°, was used to detect two breakup fragments (e.g., α-t, α-d, α-p, or α-α) in coincidence produced by either direct or sequential breakup events. Each telescope consists of two Si strip detectors, with thicknesses of $\sim$60 μm (as ΔE) and $\sim$1500 μm (as E). Each detector has 16 vertical strips in its front side and 16 horizontal strips in the back, with 256 pixels, covering an active area of 50 × 50 mm^2, with length and breadth of each strip being 50 and 3.1 mm, respectively. Two Si-surface barrier (SSB) detectors kept at ±20° were used to monitor the incident flux. In addition, there were five single telescopes (T_1–T_5) of SSB detectors (with $\Delta E \sim 50$ μm, $E \sim$ 1000–2000 μm) to measure the elastic scattering at additional angles. The typical inclusive two-dimensional energy-calibrated spectrum of ΔE vs $E_{\rm total}$ obtained from a strip telescope, given in Fig. 1, shows a good separation of the particles with different masses (A = 1–7) and charges (Z = 1–3) produced by different reaction mechanisms. An α was detected in one pixel in coincidence with any of t, d, p, and α particles in another pixel indicating the presence of direct or resonant, $-1n$ transfer, $-2n$ transfer, and $+1p$ transfer breakup, respectively. The $-1n$ and $-1p$ transfer reactions that survive post breakup produce ^{6}Li and ^{6}He, respectively. However, both ^{6}Li and ^{6}He can also be produced from the direct breakup of ^{7}Li into ^{6}Li + n and ^{6}He + p fragments respectively.

The inset of Fig. 1 shows the effective range of θ ($\sim$51°–142°) and ϕ ($\sim\pm7^\circ - \pm 11^\circ$) coverage of the strip detector array and the distribution of events corresponds to the number of α particles detected in coincidence with either t or d or p in any two vertical strips.

The relative energy $E_{\rm rel}$ of two breakup fragments [22] of each reaction event was reconstructed using the measured energies and emitting angles of two breakup fragments. The corresponding efficiencies of the detector array were obtained by a Monte Carlo simulation. The $E_{\rm rel}$ distribution enables the excitation energy of the projectile-like nucleus above its breakup threshold through which the breakup occurs to be inferred.

Monte Carlo simulations have been performed to find the efficiency of detecting two breakup fragments in coincidence by any two strips as a function of $E_{\rm rel}$. The breakup fragments were assumed to be emitted isotropically in the rest frame of the outgoing projectile-like nucleus before it broke up. The $E_{\rm rel}$ and efficiency of the detector have been determined event by event. This efficiency distribution was applied to the raw data to obtain the efficiency-corrected $E_{\rm rel}$ distribution.

For ^{7}Li breaking into α and t, the $E_{\rm rel}$ distribution without efficiency correction, the $E_{\rm rel}$-dependent efficiency of the detector array, and the $E_{\rm rel}$ distribution with efficiency correction have been shown in Figs. 2(a), 2(b) and 2(c), respectively. In the $E_{\rm rel}$ distribution of $\alpha + t$ breakup, it is interesting to observe that in addition to the direct breakup at low energy, there are two dominant peaks at $\sim$2.23 and $\sim$4.28 MeV which correspond to the first and second resonance states at $7/2^-$ (4.63 MeV) and $5/2^-$ (6.68 MeV), respectively. The shape of the distribution and the relative intensities of the two states are similar to the ones observed in Refs. [23,24]. The comparison of the peak positions and widths of resonances with literature values in Table I confirms the observation of ^{7}Li breakup into $\alpha + t$ via

TABLE I. Comparison of the observed energies and widths of the resonance peaks in relative energy distributions with the literature [25].

State	Present work		Literature	
	E_{rel} (MeV)	Γ (MeV)	E_{rel} (MeV)	Γ (MeV)
^{7}Li(7/2^{-})	2.23	0.20	2.16	0.09
^{7}Li(5/2^{-})	4.28	1.20	4.21	0.88
^{6}Li(3^{+})	0.68	0.14	0.71	0.024
^{6}Li(2^{+})	2.93	1.06	2.84	1.30
^{6}Li(1^{+})	4.50	1.29	4.18	1.50
^{5}Li(3/2^{-})	2.15	1.50	1.97	1.23

its $5/2^{-}$ resonance for the first time along with $7/2^{-}$ resonance and direct breakup.

The efficiency-corrected E_{rel} distributions have also been obtained for $\alpha + d$, $\alpha + p$, and $^{6}\mathrm{He} + p$ breakup as shown in Figs. 2(d), 2(e), and 2(f), respectively. It can be observed that for the $^{7}\mathrm{Li} \xrightarrow{-1n} {}^{6}\mathrm{Li} \rightarrow \alpha + d$ reaction, the breakup mainly proceeded with three relative energies around 0.71, 2.84, and 4.18 MeV corresponding to three resonances (3^{+}, 2^{+} and 1^{+}) of ^{6}Li (see Table I). In the E_{rel} distribution shown in Fig. 2(e) corresponding to the (^{7}Li,^{5}Li $\rightarrow \alpha + p$) reaction, the breakup was found to have proceeded only with $E_{rel} \sim 1.97$ MeV which is equal to the Q value of $^{5}\mathrm{Li}_{g.s.} \rightarrow \alpha + p$ reaction. The measured positions and widths of the peaks in E_{rel} distributions corresponding to the breakup of ^{7}Li, ^{6}Li, and ^{5}Li have been compared with the literature data [25] as shown in Table I to identify the respective resonance states.

Despite a very high breakup threshold (∼10 MeV) for $^{7}\mathrm{Li} \rightarrow {}^{6}\mathrm{He} + p$ channel, it was interesting to observe a significant number of ^{6}He-p events as shown in Fig. 2(f). For this breakup channel, the E_{rel} distribution does not have any well-defined peak and hence it can be taken as a direct (nonresonant) breakup. The ^{7}Li structure as a cluster of $^{6}\mathrm{He} + p$ is not well investigated. However, there is evidence of this structure in the observation of transfer or capture of ^{6}He from ^{7}Li by the target nuclei [26]. So, the present exclusive measurement of ^{6}He in coincidence with a proton that provides direct evidence of the $^{6}\mathrm{He} + p$ cluster structure of ^{7}Li is very important in understanding the possible cluster structures of ^{7}Li.

Next, to find out the excitations of the residual target nuclei, the Q-value distributions were also obtained using the expression of Ref. [7]. Two-dimensional plots of E_{rel} vs Q value can reveal the excitations of both projectile-like and target-like nuclei as shown in Fig. 3(a) for $\alpha + p$, $\alpha + t$, and $^{6}\mathrm{He} + p$ breakup and in Fig. 3(b) for $\alpha + d$ breakup. In the case of $\alpha + t$ breakup and $^{6}\mathrm{He} + p$ breakup, most of the events are centered around Q values equal to ∼−2.5 and ∼−10 MeV, respectively, corresponding to the ground state of ^{112}Sn. However, for $\alpha + p$ breakup, there are two distinct peaks at ∼7.1 and ∼5.8 MeV in the Q-value distribution corresponding to the ground state and first excited state (2^{+}, 1.3 MeV) of ^{114}Sn followed by a broad peak at $Q \sim 4.3$ MeV corresponding to an average excitation of ∼3 MeV of ^{114}Sn due to many closely spaced energy levels of ^{114}Sn in this region. The relative

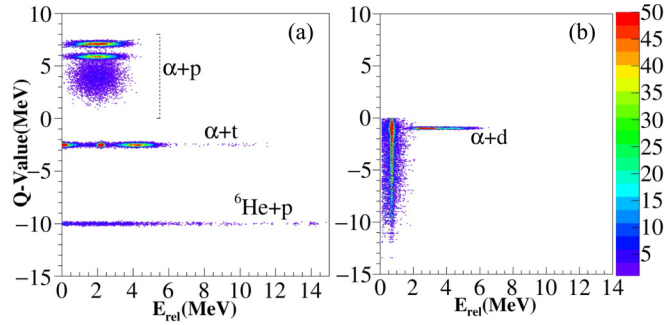

FIG. 3. Two-dimensional plot of E_{rel} vs Q value showing the distribution of events with different projectile-like and target-like excitations for (a) $\alpha + p$, $\alpha + t$, and $^{6}\mathrm{He} + p$ breakup reactions and (b) $\alpha + d$ breakup reaction.

energies for these α-p events with different Q values are all centered around 1.97 MeV which is the same as the energy released in the $^{5}\mathrm{Li}_{g.s.} \rightarrow \alpha + p$ breakup.

In the case of $\alpha + d$ breakup [see Fig. 3(b)], the maximum events were observed at $Q \sim -1.0$ MeV corresponding to the ground state of ^{113}Sn accompanied by three resonance states (3^{+}, 2^{+}, and 1^{+}) of ^{6}Li. However, there are events with excitation of ^{113}Sn up to 11 MeV which are accompanied by only the 3^{+} resonance excitation of ^{6}Li. In addition there are direct (nonresonant) breakups with relative energies in the range of 0–1.5 MeV and ^{113}Sn excitation up to ∼10 MeV. The breakup via 2^{+} and 1^{+} resonances are found to occur only with ^{113}Sn in its ground state.

For $^{7}\mathrm{Li} \rightarrow {}^{6}\mathrm{He} + p$ breakup, since the breakup threshold is very high (∼10 MeV) the number of breakup events was found to be small and they primarily occur with no excitation of target-like nuclei.

The differential cross sections for each of the measured breakup channels have been obtained as follows. Using events reconstruction for a particular breakup channel, for example, $\alpha + t$, a distribution of events corresponding to different θ,ϕ of the outgoing cluster particle just before breakup, i.e., ^{7}Li* was generated. Now, for each $\theta(^{7}\mathrm{Li}^{*})$ bin, the efficiency-corrected relative energy distribution $[Y_i^{\mathrm{eff}}(\theta) = Y_i^{\mathrm{raw}}(\theta)/\zeta_i]$ was obtained by summing over all $\phi(^{7}\mathrm{Li}^{*})$ coverage of detector array corresponding to the same $\theta(^{7}\mathrm{Li}^{*})$ bin. Here, $Y_i^{\mathrm{raw}}(\theta)$ represents the yield of the ith bin of the relative energy between ϵ_i and $\epsilon_i + d\epsilon_i$ without efficiency correction, and ζ_i is the efficiency of the detector array for the same relative energy bin. For a particular θ bin, the coincidence yields under the peaks corresponding to $7/2^{-}$ and $5/2^{-}$ resonances in E_{rel} distribution have been extracted individually by integrating $Y_i^{\mathrm{eff}}(\theta)$ in steps of $d\epsilon_i$ over the respective E_{rel} range ($\Delta\epsilon = N d\epsilon_i$). Differential breakup cross sections for each of the resonance states are extracted from the following relation:

$$\frac{d\sigma^{\mathrm{br}}}{d\Omega}(\theta) = \frac{\sum_{i=1}^{N} Y_i^{\mathrm{eff}}(\theta)}{Y_{\mathrm{el}}(\theta)} \frac{d\sigma^{\mathrm{el}}}{d\Omega}(\theta), \tag{1}$$

where $Y_{\mathrm{el}}(\theta)$ is the yield of elastic scattering in the solid angle corresponding to the elements $\Delta\theta(^{7}\mathrm{Li}^{*})$ and $\Delta\phi(^{7}\mathrm{Li}^{*})$, and $\frac{d\sigma^{\mathrm{el}}}{d\Omega}(\theta)$ is the differential elastic scattering cross section. The latter was obtained by normalizing (i) $Y_{\mathrm{el}}(\theta)$ to the monitor

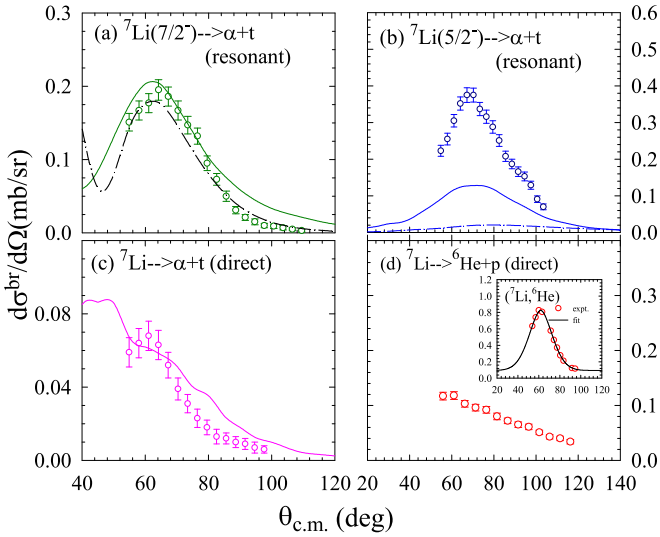

FIG. 4. Cross sections for sequential breakup of $^7\mathrm{Li} \rightarrow \alpha + t$ for its (a) $7/2^-$ and (b) $5/2^-$ resonances, respectively; (c) direct breakup of $^7\mathrm{Li} \rightarrow \alpha + t$ and (d) direct breakup of $^7\mathrm{Li} \rightarrow {}^6\mathrm{He} + p$. The lines represent the results of CDCC calculations.

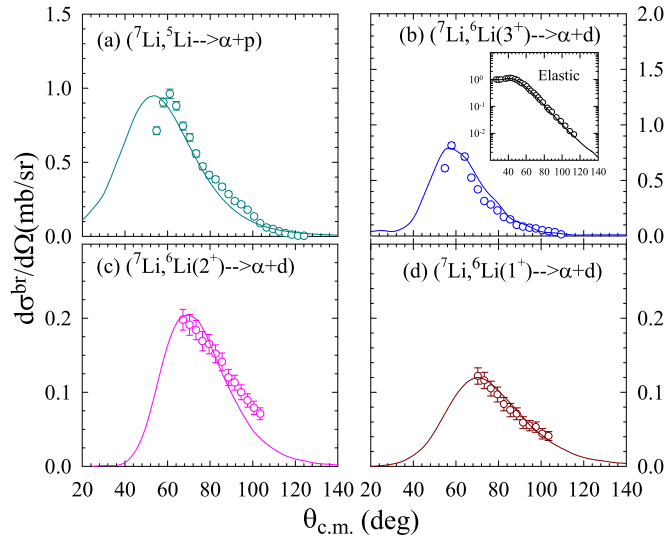

FIG. 5. Cross sections for (a) sequential breakup of $^7\mathrm{Li} \xrightarrow{-2n} {}^5\mathrm{Li} \rightarrow \alpha + p$ and (b-d) sequential breakup of $^7\mathrm{Li} \xrightarrow{-1n} {}^6\mathrm{Li} \rightarrow \alpha + d$ through 3^+, 2^+ and 1^+ resonance states of ^{6}Li respectively. The elastic scattering data are shown as an inset of panel (b). Solid lines represent the results of CRC calculations.

yield $Y_m(\theta_m)$ corresponding to Rutherford scattering and (ii) their solid angles. Thus, the cross sections for the $^7\mathrm{Li} \rightarrow \alpha + t$ breakup via $7/2^-$ and $5/2^-$ resonances have been obtained and shown as hollow circles in Figs. 4(a) and 4(b). The cross section for the direct breakup of $^7\mathrm{Li} \rightarrow \alpha + t$ with relative energy in the range of 0–0.5 MeV is shown in Fig. 4(c). Although the breakup cross section via $7/2^-$ resonance has been measured and described earlier using different targets, the cross section for $5/2^-$ resonance is measured for the first time.

Similarly, the cross sections for direct breakup of ^{7}Li into ^{6}He and p, which is again measured for the first time, has been shown in Fig. 4(d). The cross section for the (^{7}Li,^{6}He) transfer reaction corresponding to $Q_{gg} = -6.9$ MeV has also been shown as an inset to Fig. 4(d), and found to be much larger than for the $^6\mathrm{He} + p$ breakup.

The cross sections for the breakup of $^7\mathrm{Li} \xrightarrow{-2n} {}^5\mathrm{Li} \rightarrow \alpha + p$ via the ground state of ^{5}Li are shown in Fig. 5(a). Similarly, the ones for $1n$ stripping followed by breakup into $\alpha + d$ through 3^+, 2^+, and 1^+ resonances of ^{6}Li are shown in Figs. 5(b), 5(c) and 5(d), respectively. The elastic scattering angular distribution used for obtaining potential parameters (required for coupled-channel calculations) has also been shown as an inset of Fig. 5(b). The lines in Figs. 4 and 5 represent the results of the coupled-channel calculations described in the following section.

Breakup cross sections for $^7\mathrm{Li} \rightarrow \alpha + t$ have been calculated by the continuum discretized coupled-channel (CDCC) method using FRESCO [27], similar to Ref. [28]. The cluster-folded (CF) interaction was used, where Sao-Paolo potentials [29] multiplied by 0.65 were taken as the real parts of the fragment-target ($\alpha + {}^{112}\mathrm{Sn}$ and $t + {}^{112}\mathrm{Sn}$) potentials. The imaginary potential for $\alpha + {}^{112}\mathrm{Sn}$ was taken from Ref. [30] including both volume and surface terms, and for $t + {}^{112}\mathrm{Sn}$ it was calculated from global optical model [31]. The α-t binding potentials of Ref. [32] were suitably modified for resonances. The spectroscopic amplitude of α-t was taken to be 0.7 for each of the excited states of ^{7}Li. The CDCC calculations for $\alpha + t$ breakup using the above parameters, shown as solid lines in Fig. 4(a)–4(c), reasonably reproduce the experimental cross sections for the $7/2^-$ resonant state and direct breakup (with $E_{\mathrm{rel}} \leqslant 0.5$ MeV). However, the cross sections calculated for $5/2^-$ resonant state at 6.67 MeV (solid line) are much smaller than the experimental values. Using the α-t binding potentials from Ref. [17] the cross sections for the $5/2^-$ state are even smaller (dash-dot line) though the $7/2^-$ state and elastic scattering are explained well. The enhanced experimental cross section for the $5/2^-$ state could be due to the contribution coming from other states overlapping with the same excitation energies. The width of the $5/2^-$ state being much larger (∼1.2 MeV) than for the $7/2^-$ state (∼0.2 MeV), the yield under the $5/2^-$ peak can have some contributions from nonresonant breakup with the same relative energies but different L values. In addition, the contribution from another $5/2^-$ resonant state at 7.46 MeV [25,33], though small, could be present. In fact, a larger cross section for the $5/2^-$ state than for the $7/2^-$ state has also been observed in the case of resonance scattering of ^{4}He from ^{3}H by Spiger and Tombrello [23] and Ivanovich *et al.* [24].

For $-1n$ and $-2n$ transfer induced breakup channels, the coupled reaction channel (CRC) calculations using FRESCO have been compared with the measured $\alpha + d$ and $\alpha + p$ breakup cross sections, respectively. After $1n$ stripping from the projectile ^{7}Li to the target ^{112}Sn, when ^{6}Li is formed in an excited state above the α-d breakup threshold, it immediately breaks up into an α-d pair. So only the resonance states of ^{6}Li were considered. For the entrance channel of the CRC calculation scheme, the real and imaginary potentials of the Woods-Saxon volume form with $V_0 = 25.33$ MeV, $r_0 = 1.185$ fm, $a_0 = 0.75$ fm, $W = 25.38$ MeV, $r_W = 1.17$ fm, and

TABLE II. Experimental and/or calculated cross sections for different outgoing channels in $^{7}\mathrm{Li} + ^{112}\mathrm{Sn}$ reaction at $E_{\mathrm{beam}} = 30$ MeV ($E_{\mathrm{cm}}/V_{\mathrm{b}} \simeq 1.37$).

Reaction channel	σ^{expt}(mb)	σ^{cal}(mb)
$^{7}\mathrm{Li} \rightarrow {}^{6}\mathrm{Li}^{*}(3^{+}) \rightarrow \alpha + d$ (res.)	2.36 ± 0.24	2.49
$^{7}\mathrm{Li} \rightarrow {}^{6}\mathrm{Li}^{*}(2^{+}) \rightarrow \alpha + d$ (res.)	0.87 ± 0.10	0.80
$^{7}\mathrm{Li} \rightarrow {}^{6}\mathrm{Li}^{*}(1^{+}) \rightarrow \alpha + d$ (res.)	0.54 ± 0.06	0.55
$^{7}\mathrm{Li}^{*}(7/2^{-}) \rightarrow \alpha + t$ (res.)	0.77 ± 0.20	0.82[a](0.72[b])
$^{7}\mathrm{Li}^{*}(5/2^{-}) \rightarrow \alpha + t$ (res.)	1.73 ± 0.20	0.69[a](0.16[b])
$^{7}\mathrm{Li} \rightarrow {}^{6}\mathrm{He} + p$ (direct)	0.74 ± 0.10	
$^{7}\mathrm{Li} \rightarrow {}^{5}\mathrm{Li} \rightarrow \alpha + p$	3.71 ± 0.37	3.10
(^{7}Li,^{6}He) for g.s.	3.11 ± 0.3	
Inclusive α	288 ± 25	
Fusion (Bass model)		864
Reaction (from OM fit)	1230 ± 20	1208

[a]α-t binding potential [32].
[b]α-t binding potential [17].

$a_W = 0.787$ fm, obtained from the fit to the measured elastic scattering, were used. For the exit channels, the real potentials are the same as above but the imaginary potentials were taken to be of short-range and Woods-Saxon square forms. The 3^{+} state of ^{6}Li was coupled to the ground plus six excited states of ^{113}Sn, whereas the 2^{+} and 1^{+} states of ^{6}Li were coupled only to the ground state of ^{113}Sn because experimentally it was observed that the breakups of 2^{+} and 1^{+} states are accompanied by only the ground-state excitation of ^{113}Sn. The spectroscopic amplitudes for $\langle {}^{112}\mathrm{Sn} + n | {}^{113}\mathrm{Sn} \rangle$ corresponding to seven states of ^{113}Sn with $E_x = 0$–1.556 MeV are taken from Ref. [34]. Spectroscopic amplitudes for $\langle {}^{7}\mathrm{Li} | {}^{6}\mathrm{Li}_{2.18\,\mathrm{MeV}} + n \rangle$, $\langle {}^{7}\mathrm{Li} | {}^{6}\mathrm{Li}_{4.31\,\mathrm{MeV}} + n \rangle$, and $\langle {}^{7}\mathrm{Li} | {}^{6}\mathrm{Li}_{5.65\,\mathrm{MeV}} + n \rangle$ are optimized at 0.605, 0.905, and 1.205, respectively, to reproduce the experimental cross sections.

For dineutron stripping, the ejectile ^{5}Li being a quasibound nucleus breaks into α and p. Hence, the cross section for $-2n$ transfer calculated from CRC calculations is equal to the $\alpha + p$ breakup cross section. From the Q-value distribution it was observed that a one-step transfer process is dominating, so only direct stripping of $2n$ from ^{7}Li has been considered in the calculations. Again, the entrance and exit channel real potentials are the same. The imaginary potential in the exit channel is short ranged. In the couplings, the g.s. of ^{5}Li and g.s. plus first excited state of ^{114}Sn have been included. The spectroscopic amplitudes $\langle {}^{7}\mathrm{Li} | {}^{5}\mathrm{Li} + 2n \rangle$ and $\langle {}^{114}\mathrm{Sn} | {}^{112}\mathrm{Sn} + 2n \rangle$ are taken to be 1.0. The calculations represented by solid lines in Fig. 5 reproduce the experimental data reasonably well.

A comprehensive list of experimental (estimated from angular distribution) and/or theoretical cross sections corresponding to different channels, along with total reaction cross sections obtained from the optical model fit to elastic scattering, is given in Table II.

In summary, exclusive measurements for various breakup channels consisting of both direct and sequential modes have been carried out using a large strip detector array for the $^{7}\mathrm{Li} + ^{112}\mathrm{Sn}$ system at a bombarding energy of 30 MeV. The sequential breakup of ^{7}Li into $\alpha + t$ through its second resonance state ($5/2^{-}$) has been measured for the first time along with its first resonance state ($7/2^{-}$). Two more dominating sequential breakup modes were found to proceed through transfer channels, i.e., (i) $^{7}\mathrm{Li} \xrightarrow{-1n} {}^{6}\mathrm{Li} \rightarrow \alpha + d$ and (ii) $^{7}\mathrm{Li} \xrightarrow{-2n} {}^{5}\mathrm{Li} \rightarrow \alpha + p$, where one of the breakup fragments is α. Thus, the results on direct, resonant, and transfer breakup of ^{7}Li by ^{112}Sn presented here provide a good foundation toward the comprehensive understanding of the reaction mechanisms of the projectile breakup as well as the production of large inclusive α in a reaction involving a weakly bound stable or unstable light projectile.

Further, the observation of direct breakup of ^{7}Li into ^{6}He and p for the first time provides direct evidence of a $^{6}\mathrm{He} + p$ cluster structure for ^{7}Li. The present result will initiate refined theoretical modeling by including an additional cluster combination to understand the complete structure of ^{7}Li and its energy levels.

S.S. and D.C. acknowledge the financial support of BRNS through the DAE-SRC Project No. "2012/21/11-BRNS/1090".

[1] L. F. Canto, P. R. S. Gomes, R. Donangelo, and M. S. Hussein, Phys. Rep. **424**, 1 (2006).
[2] N. Keeley, N. Alamanos, K. W. Kemper, and K. Rusek, Prog. Part. Nucl. Phys. **63**, 396 (2009).
[3] J. J. Kolata, V. Guimaraes, and E. Aguilera, Eur. Phys. J. A **52**, 123 (2016).
[4] B. B. Back, H. Esbensen, C. L. Jiang, and K. E. Rehm, Rev. Mod. Phys. **86**, 317 (2014).
[5] D. Chattopadhyay, S. Santra, A. Pal, A. Kundu, K. Ramachandran, R. Tripathi, D. Sarkar, S. Sodaye, B. K. Nayak, A. Saxena *et al.*, Phys. Rev. C **94**, 061602(R) (2016).
[6] S. K. Pandit, A. Shrivastava, K. Mahata, N. Keeley, V. V. Parkar, P. C. Rout, K. Ramachandran, I. Martel, C. S. Palshetkar, A. Kumar *et al.*, Phys. Rev. C **93**, 061602(R) (2016).
[7] D. H. Luong, M. Dasgupta, D. J. Hinde, R. du Rietz, R. Rafiei, C. J. Lin, M. Evers, and A. Diaz-Torres, Phys. Rev. C **88**, 034609 (2013).
[8] S. Santra, V. V. Parkar, K. Ramachandran, U. K. Pal, A. Shrivastava, B. J. Roy, B. K. Nayak, A. Chatterjee, R. K. Choudhury, and S. Kailas, Phys. Lett. B **677**, 139 (2009).
[9] K. O. Pfeiffer, E. Speth, and K. Bethge, Nucl. Phys. A **206**, 545 (1973).
[10] F. Souza, C. Beck, N. Carlin, N. Keeley, R. L. Neto, M. de Moura, M. Munhoz, M. D. Santo, A. Suaide *et al.*, Nucl. Phys. A **821**, 36 (2009).
[11] D. Scholz, H. Gemmeke, L. Lassen, R. Ost, and K. Bethge, Nucl. Phys. A **288**, 351 (1977).
[12] A. Shrivastava, A. Navin, N. Keeley, K. Mahata, K. Ramachandran, V. Nanal, V. Parkar, A. Chatterjee, and S. Kailas, Phys. Lett. B **633**, 463 (2006).
[13] C. Signorini, A. Edifizi, M. Mazzocco, M. Lunardon, D. Fabris, A. Vitturi, P. Scopel, F. Soramel, L. Stroe *et al.*, Phys. Rev. C **67**, 044607 (2003).
[14] C. M. Castaneda, H. A. Smith, P. P. Singh, and H. Karwowski, Phys. Rev. C **21**, 179 (1980).

[15] F. A. Souza, N. Carlin, C. Beck, N. Keeley, A. Diaz-Torres, R. L. Neto, C. Siqueira-Mello, M. M. de Moura, M. G. Munhoz, R. A. N. Oliveira *et al.*, Nucl. Phys. A **834**, 420c (2010).
[16] C. Beck, N. Rowley, P. Papka, S. Courtin, M. Rousseau, F. A. Souza, N. Carlin, R. L. Neto, M. M. de Moura, M. G. D. Santo *et al.*, Nucl. Phys. A **834**, 440c (2010).
[17] A. Diaz-Torres, I. J. Thompson, and C. Beck, Phys. Rev. C **68**, 044607 (2003).
[18] K. Rusek, P. D. Cathers, E. E. Bartosz, N. Keeley, K. W. Kemper, and F. Marechal, Phys. Rev. C **67**, 014608 (2003).
[19] W. Ott, R. Butsch, H. J. Jansch, K.-H. Mobius, P. Paul, G. Tungate, and E. Steffens, Nucl. Phys. A **489**, 329 (1988).
[20] V. Mihailovic and M. Poljsak, Nucl. Phys. A **311**, 377 (1978).
[21] S. Santra, S. Kailas, V. V. Parkar, K. Ramachandran, V. Jha, A. Chatterjee, P. K. Rath, and A. Parihari, Phys. Rev. C **85**, 014612 (2012).
[22] R. J. de Meijer and R. Kamermans, Rev. Mod. Phys. **57**, 147 (1985).
[23] R. J. Spiger and T. A. Tombrello, Phys. Rev. **163**, 964 (1967).
[24] M. Ivanovich, P. G. Young, and G. G. Ohlsen, Nucl. Phys. A **110**, 441 (1968).
[25] D. R. Tilley, C. M. Cheves, J. L. Godwin, G. M. Hale, H. M. Hofmann, J. H. Kelley, C. G. Sheu, and H. R. Weller, Nucl. Phys. A **708**, 3 (2002).
[26] A. Shrivastava, A. Navin, A. Diaz-Torres, V. Nanal, K. Ramachandran, M. Rejmund, S. Bhattacharyya, A. Chatterjee, S. Kailas, A. Lemasson *et al.*, Phys. Lett. B **718**, 931 (2013).
[27] I. J. Thompson, Comput. Phys. Rep. **7**, 167 (1988).
[28] C. Beck, N. Keeley, and A. Diaz-Torres, Phys. Rev. C **75**, 054605 (2007).
[29] L. C. Chamon, B. V. Carlson, L. R. Gasques, D. Pereira, C. De Conti, M. A. G. Alvarez, M. S. Hussein, M. A. Cândido Ribeiro, E. S. Rossi, Jr., and C. P. Silva, Phys. Rev. C **66**, 014610 (2002).
[30] M. Avrigeanu and V. Avrigeanu, Phys. Rev. C **73**, 038801 (2006).
[31] X. Li, C. Liang, and C. Cai, Nucl. Phys. A **789**, 103 (2007).
[32] B. Buck *et al.*, J. Phys. G: Nucl. Part. Phys. **14**, L211 (1988).
[33] F. Ajzenberg-Selove, Nucl. Phys. A **490**, 52 (1988).
[34] E. J. Schneid, A. Prakash, and B. L. Cohen, Phys. Rev. **156**, 1316 (1967).